Spectral analysis of the complex cubic oscillator

2000 J. Phys. A: Math. Gen. 33 8771

(http://iopscience.iop.org/0305-4470/33/48/314)

J. Phys. A: Math. Gen. **33** (2000) 8771–8796. Printed in the UK PII: S0305-4470(00)11844-X

Spectral analysis of the complex cubic oscillator

Eric Delabaere† and Duc Tai Trinh‡

† Département de Mathématiques, UMR CNRS 6093, Université d'Angers, 2 Boulevard Lavoisier, 49045 Angers Cedex 01, France
‡ Department of Mathematics, College of Dalat, 29 Yersin, Dalat, Vietnam

E-mail: delab@tonton.univ-angers.fr and tductai@hcm.vnn.vn

Received 14 February 2000, in final form 20 September 2000

Abstract. Using the 'exact semiclassical analysis', we study the spectrum of a one-parameter family of complex cubic oscillators. The $\mathcal{PT}$-invariance property of the complex Hamiltonians and the reality property of the spectrum are discussed. Analytic continuations of the spectrum in the complex parameter and their connections with the resonance problem for the real cubic oscillator are investigated. The global analytic structure of the spectrum yields a branch point structure similar to the multivalued analytic structure discovered by Bender and Wu for the quartic oscillator.

1. Introduction

Quantum systems characterized by non-Hermitian Hamiltonians are known to be of particular interest in theoretical physics, e.g. quantum field theory and nuclear physics (see [1, 2] and references therein). The purpose of this paper is to contribute to the subject, with a conjecture of Bessis and Zinn-Justin [3, 4] and recent works on complex operators with real spectra ([5], for instance) as a more precise motivation.

A large class of examples of one-dimensional Schrödinger Hamiltonians $\mathcal{H} = p^2 + V(q)$, $p = -\mathrm{i}\mathrm{d}/\mathrm{d}q$ with complex-valued potentials $V(q)$ but exhibiting real spectra are now known. Most of these examples (cf [1, 3, 6–9]) share the property of enjoying $\mathcal{PT}$-invariance§, where $\mathcal{P} : (p, q) \mapsto (-p, -q)$ is the parity operator and $\mathcal{T} : (p, q) \mapsto (-\overline{p}, \overline{q})$ is the time-reversal operator, i.e. the potential satisfies the functional equality $\overline{V(-\overline{q})} = V(q)$. It is commonly believed that the existence of real spectra for such Hamiltonians proceeds directly from the $\mathcal{PT}$-invariance property.

Such a belief may be enforced by the works of Caliceti *et al* [11, 12] (see also [13]), and more recently [14], where a class of odd anharmonic oscillators $H_\beta = p^2 + q^2 + \beta q^{2N+1}$ (N is a positive integer) is studied, indeed $\mathcal{PT}$-symmetric for pure imaginary β. When $\mathrm{Im}(\beta) > 0$ (respectively, $\mathrm{Im}(\beta) < 0$), H_β has a compact resolvant (and hence has no continuous spectrum) and, furthermore, has a non-empty spectrum, with real eigenvalues when β is pure positive (respectively, negative) imaginary, at least for $|\beta|$ small enough. This last result was also proved (using a different method) in [4] in the $N = 1$ case, which corresponds to the Bessis–Zinn-Justin conjecture.

§ Nevertheless, $\mathcal{PT}$-symmetry is not a necessary condition (see [10] for instance).

0305-4470/00/488771+26$30.00

Following the announcement of the note [4], our purpose is to keep on our investigation of this last Bessis–Zinn-Justin case. However, instead of working with the above Hamiltonian H_β (and $N = 1$), it will be more convenient to work with the family of Hamiltonians

$$\mathcal{H}_\alpha = p^2 + \mathrm{i}q^3 + \mathrm{i}\alpha q \tag{0}$$

which is $\mathcal{PT}$-symmetric for real α. It appears that the situation is quite different depending on whether α is positive or not. To the case α real positive ($|\alpha|$ large) in this representation corresponds $\beta = \mathrm{i}(3\alpha)^{-5/8}$ pure positive imaginary ($|\beta|$ small) in Caliceti *et al*'s model: from [4, 13] and for $\alpha > 0$ large enough, considering the Hamiltonian $\mathcal{H}_\alpha$ as an operator in the Hilbert space L^2, we thus obtain a discrete spectral set of real eigenvalues, with analytic dependence with respect to α. As we shall see, such a property is actually destroyed when α becomes negative, where pairs of (real) eigenvalues degenerate before becoming complex conjugate: as noted in [15], the $\mathcal{PT}$-symmetry property is not a sufficient demand to ensure real spectra.

This result becomes more understandable when some analytic continuations are performed in the complex α-plane. A particular interesting feature occurs when the phase of α reaches the $\mp 4\pi/5$ values, which corresponds to β *real* in Caliceti *et al*'s perturbative model: the analytic continuations of the eigenvalues are directly related to *resonance values* (or their complex conjugate, depending on the sign $\mp$) of the *real* cubic oscillator. As pointed out in [11], this yields a natural notion of resonance, viewed as analytic continuations of bound states.

The investigation of the quantization condition near the top of the cubic barrier gives the key to a beautiful multivalued analytic structure of the analytic continuations of the spectrum, in complete analogy with the complex branch point structure discovered by Bender and Wu [16] for the quartic oscillator and much analysed since [17–19]: *the eigenvalues are only determinations of a* sole *multivalued function with a quasi-lattice of square root branch points for its singularities*.

This multivalued analytic structure can be investigated by the same techniques as those used in [19] to analyse the conjecture of Bender and Wu. Considering α as a large (complex) parameter, we shall make constant use of the 'exact WKB analysis' developed in [20, 21], after ideas introduced by Voros [22, 23] and Ecalle [24]. The efficiency of this powerful tool has an unfortunate counterpart: from the theoretical side, our analysis will only be valid for $|\alpha|$ large enough. Nevertheless, our belief is that the 'unknown zone' where our method does not apply does not hold particularly surprising phenomena. Some of the following claims (section 2) are derived from this belief. We shall make precise in the following sections (section 4 and 5) to what extent these claims can be considered as rigorous results.

2. Main claims

We start with $\alpha > 0$ and consider $\mathcal{H}_\alpha$ as an operator in the Hilbert space $L^2(\mathbb{R})$. Then:

Claim 1. *For α positive real, the spectrum of $\mathcal{H}_\alpha$ consists in a discrete set of eigenvalues $E_n(\alpha)$, $n \in \mathbb{N}$ depending on α as real analytic functions.*

Consequently, we claim that the Bessis–Zinn-Justin conjecture is true, at least when positive real α are concerned. For any positive integer n, the eigenvalue $E_n(\alpha)$ is asymptotic to $\frac{2}{3\sqrt{3}}\alpha^{3/2}$ when $\alpha \to +\infty$, and more precisely:

Claim 2. *For all $n = 0, 1, \ldots$, the eigenvalue E_n is asymptotic to the Rayleigh–Schrödinger series*

$$E_n(\alpha) \sim \frac{2}{3\sqrt{3}}\alpha^{3/2} + \alpha^{1/4}\left(\sum_{k=0}^{\infty} E_{n,k}\alpha^{-5k/4}\right)$$

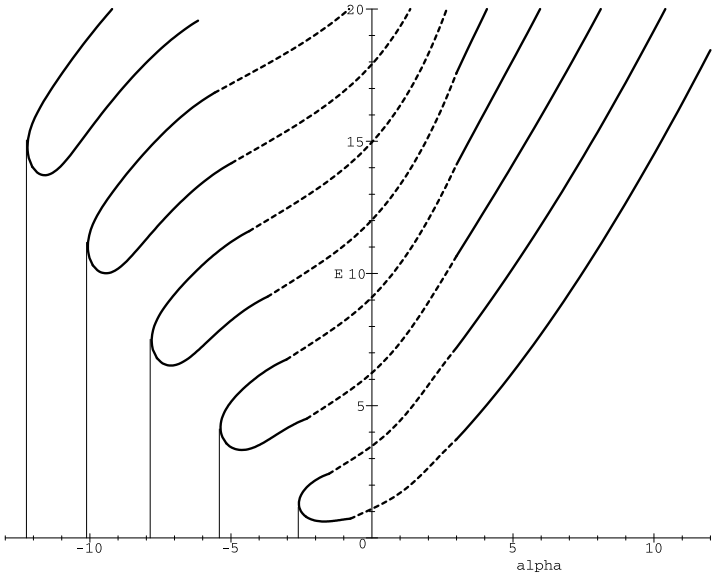

Figure 1. Bound states for real α.

where

$$E_{n,0} = 3^{1/4}(2n+1)$$
$$E_{n,1} = \tfrac{5}{8}n^2 + \tfrac{5}{8}n + \tfrac{11}{48}$$
$$E_{n,2} = -3^{-1/4}\left(\tfrac{235}{384}n^3 + \tfrac{705}{256}n^2 + \tfrac{545}{768}n + \tfrac{155}{768}\right)$$
$$\vdots$$
$$E_{n,k} \sim (-1)^{k+1}\frac{3^{1/4}\sqrt{30}}{\pi^{3/2}}60^n\left(\frac{3^{-1/4}5}{8}\right)^k\frac{\Gamma(n+k+\frac{1}{2})}{\Gamma(n+1)} \qquad (k \to +\infty).$$

Conversely, this Rayleigh–Schrödinger series is Borel resummable *with respect to* $\alpha^{5/4}$*, and its Borel sum is exactly the eigenvalue* E_n*.*

Investigations along the negative real axis give a quite different situation, showing that $\mathcal{PT}$-symmetry is not a sufficient demand to give a real spectrum: figure 1 shows that E_n have some degenerate points where E_n cross by pairs before splitting into pairs of complex conjugate eigenvalues. Precisely:

Claim 3. *For all* $k \in \mathbb{N}$*,* $E_{2k}(\alpha)$ *and* $E_{2k+1}(\alpha)$ *can be extended analytically along the negative real axis up to a common crossing point* α_k*.*

As a matter of fact this set of crossing points is only the emerged set in the real part of a quasi-lattice of singularities embedded in the complex α-plane. The complete picture reveals a Bender and Wu-like complex branch point structure!

Claim 4. $E_n(\alpha)$ *extend analytically in the* α*-complex plane as branches of a sole multivalued analytic function* $\mathbb{E}(\alpha)$*, with no singularities in* $\mathbb{C}$ *other than square root branch points.*

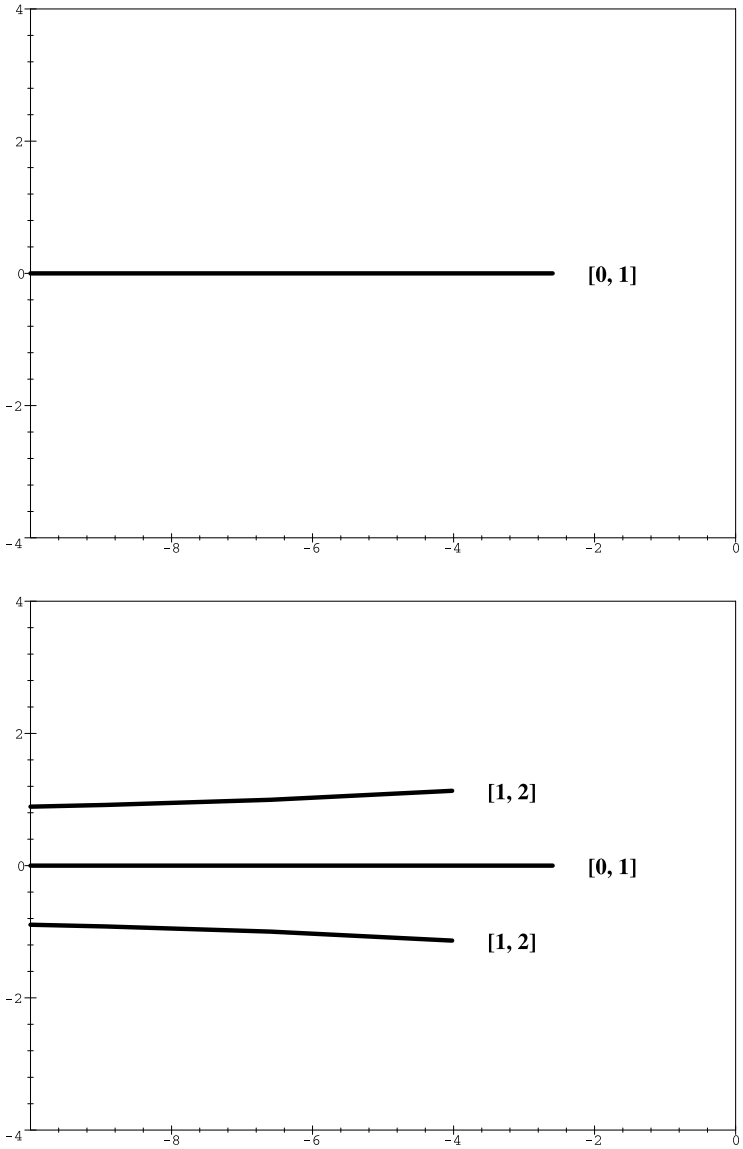

Figure 2. Westbound description for E_0 (top) and E_1 (bottom).

The Riemann surface of $\mathbb{E}(\alpha)$ can be understood by describing its different (infinite number of) sheets. This essentially means defining the different determinations $E_n(\alpha)$ of $\mathbb{E}(\alpha)$ as univalued functions defined in convenient cut planes. The simplest choice of cuts is given by what we call the 'westbound' description as shown in figures 2 and 3, with almost horizontal cuts asymptotic at infinity to the negative real axis.

In order to specify this choice of cuts, let us denote by E_n^W the 'west'-determination of (the analytic continuations of) E_n: in figures 2 and 3, the reference $[i, j]$ near a branch point means that this branch point is a common degenerate point for both E_i^W and E_j^W.

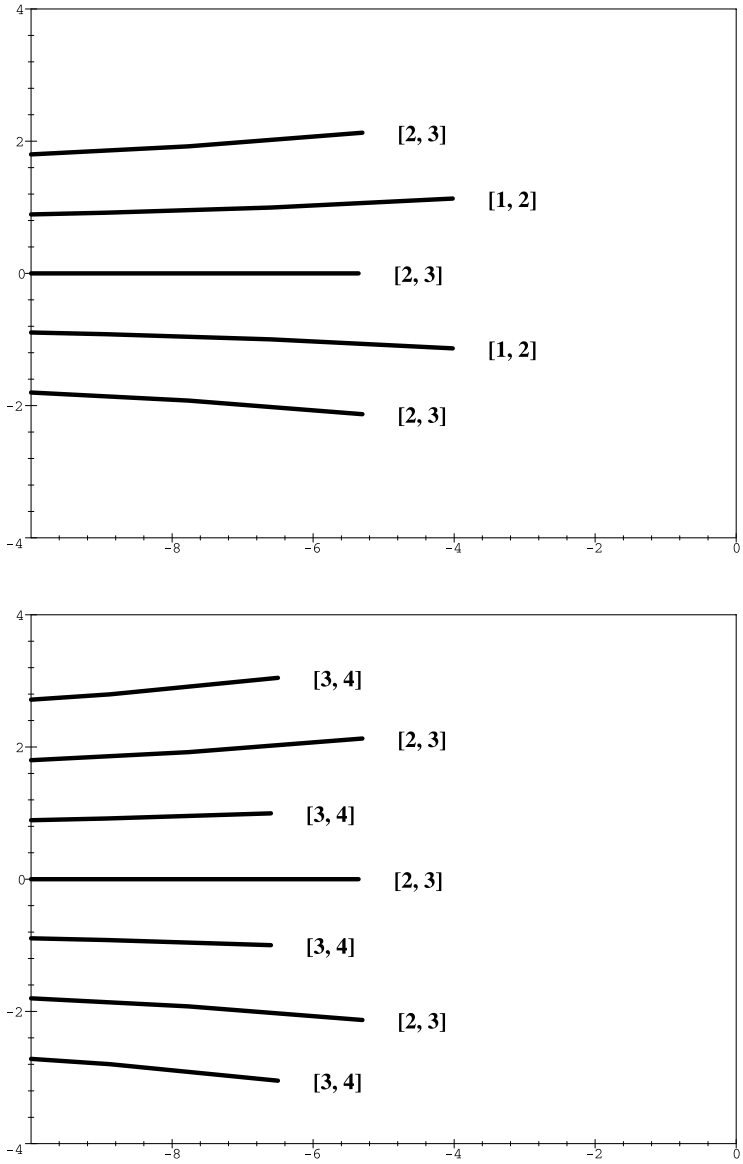

Figure 3. Westbound description for E_2 (top) and E_3 (bottom).

From these two figures, one can easily infer the following general rule: the nth west sheet has a set of $2n+1$ cuts, where n (respectively, $n+1$) of these cuts emanate from branch points which are common for E_n^W and E_{n-1}^W (respectively, E_n^W and E_{n+1}^W).

Now projecting onto the complex plane the whole set of branch points, one obtains a quasi-lattice of singularities, shown in figure 4, which is symmetric with respect to the real axis (as a consequence of the reality properties of $E_n(\alpha)$), which is confined within a single sector:

Claim 5. *The projections of all branch points belong to a sector of aperture* $\arg(\alpha) \in]4\pi/5, 6\pi/5[\bmod 2\pi$.

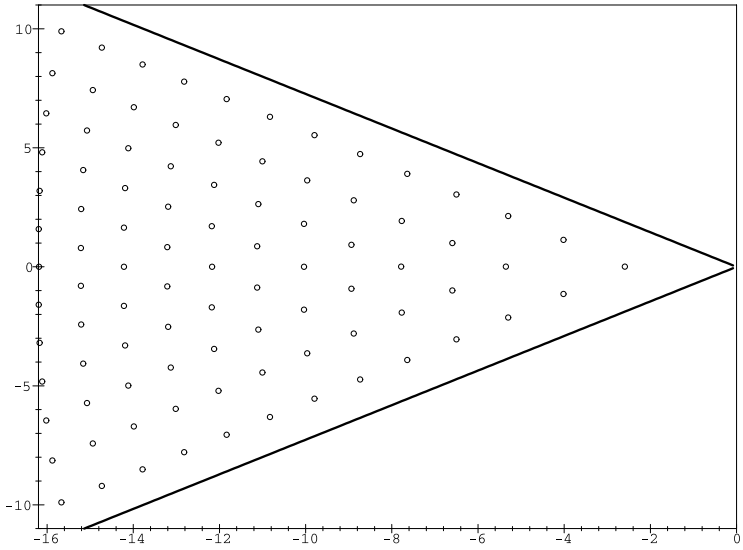

Figure 4. The quasi-lattice of singularities.

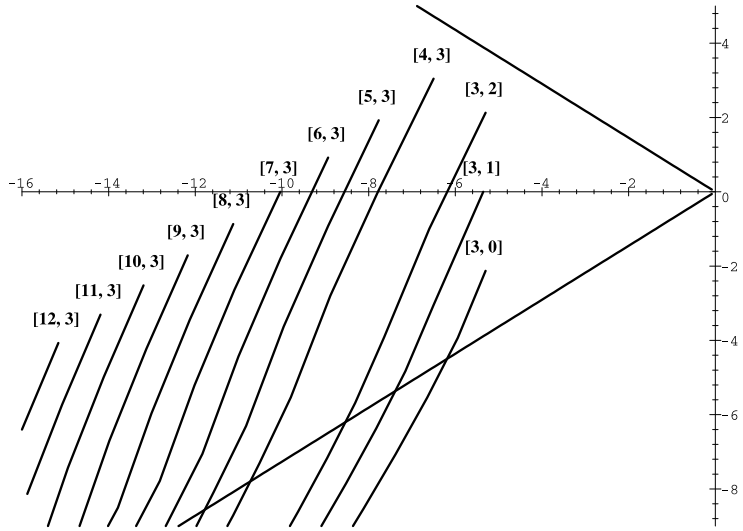

Figure 5. South-westbound description for E_3.

Returning now to $E_n(\alpha)$, one has the following property.

Claim 6. *Each $E_n(\alpha)$ can be analytically continued in a whole sectorial neighbourhood of infinity S_n of aperture $12\pi/5$,*

$$S_n := \{z = |z| \exp(\mathrm{i}\theta) \in \mathbb{C}, -6\pi/5 < \theta < 6\pi/5, |z| > r_n(\theta)\}$$

where r_n is a positive function, depending on n. Moreover, E_n is asymptotic to its Rayleigh–Schrödinger series at infinity inside the sector S_n.

At first sight, compared with claim 5 or with our description of the Riemann surface of $\mathbb{E}$, this claim 6 may appear surprising. To understand this result, one has to keep in

mind that the description of a set of sheets is a matter of choice of cuts: for instance, our 'westbound' description may be changed into the 'south-west' description as exemplified in figure 5, a suitable description when one wants to perform analytic continuations anticlockwise around the origin. We shall denote by E_n^{SW} the 'south-west' determination of (the analytic continuations of) E_n, the reference $[i, j]$ near each branch point in figure 5 meaning here again that this branch point is a common degenerate point for E_i^{SW} and E_j^{SW}.

Such a 'south-west' description (however, equivalent to the 'west' description) is now in perfect agreement with our claim 6: each E_n^{SW} reveals an infinite number of cuts emanating from a set of branch points which lie asymptotically at infinity along the direction of phase $6\pi/5$. The symmetric picture occurs for the 'north-west' description, thus giving claim 6 in its complete form.

3. Method of investigation

As pointed out by Simon [17], interesting information can be derived from the scaling (Symanzik) properties of the operator (0). Indeed, starting with the Sturm–Liouville equation

$$-\frac{\mathrm{d}^2}{\mathrm{d}q^2}\Phi + (\mathrm{i}q^3 + \mathrm{i}\alpha q)\Phi = E\Phi \tag{1}$$

the change of variables

$$q_{resc} = \hbar^{2/5} q \qquad \alpha\hbar^{4/5} = \mathrm{e}^{\mathrm{i}\theta} \qquad \widehat{E} = \hbar^{6/5} E$$

yields the following equivalent Schrödinger equation (with the abuse of notation of replacing q_{resc} by q for simplicity):

$$-\hbar^2 \frac{\mathrm{d}^2}{\mathrm{d}q^2}\Psi + (\mathrm{i}q^3 + \mathrm{i}\mathrm{e}^{\mathrm{i}\theta} q)\Psi = \widehat{E}\Psi. \tag{2}$$

Now thinking of α as a large parameter in equation (1) makes the scale parameter $\hbar$ appearing as a small parameter of the singular perturbation in equation (2). This makes the use of the (complex) WKB method possible, or more precisely its 'exact semiclassical' version [22] for which we shall refer to [20, 21].

Let us introduce some notation. For a given value of $(\theta, \widehat{E})$ we shall denote by $\mathcal{L}_{\theta,\widehat{E}}$ the (complexified) Lagrangian curve in the phase space, i.e. the curve in the (p, q)-plane defined by the equation $p^2 + \mathrm{i}q^3 + \mathrm{i}\mathrm{e}^{\mathrm{i}\theta} q = \widehat{E}$. With the projection on the complex q-plane, $\mathcal{L}_{\theta,\widehat{E}}$ can be considered as a twofold covering of $\mathbb{C}$, ramified at the *turning points* where $p = 0$.

For the formal side, we shall make constant use of the so-called *WKB expansions*. Defined *locally* on the above covering, the *WKB solutions* are formal solutions of equations (2) of the form

$$P(q, \hbar^2)^{-1/2} \exp\left(\frac{\mathrm{i}}{\hbar}\int_{q_o}^{q} P(q', \hbar^2)\,\mathrm{d}q'\right)$$

where

$$P(q, \hbar^2) = p(q) + p_1(q)\hbar^2 + p_2(q)\hbar^4 + \cdots \tag{3}$$

is a formal power series in $\hbar^2$. Such a WKB solution is, however, defined only *up to an arbitrary normalization factor*. Therefore, analytic continuation along any *closed* path γ of the covering multiplies them by a factor which does not depend on the initial normalization point q_o: we call it the *monodromy factor* of γ.

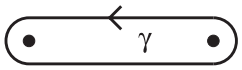

Figure 6. An example of a cycle γ.

Such a closed path, which can be thought of as a *cycle* by forgetting the base point q_o, has been drawn in figure 6. Assuming that the turning points are *simple*, i.e. are simple zeros of $\widehat{E} - (\mathrm{i}q^3 + \mathrm{i}\mathrm{e}^{\mathrm{i}\theta}q)$, and noticing that analytic continuation along γ multiplies $P(q,\hbar^2)^{-1/2}$ by -1, one sees that the monodromy factor of γ reads as $-a^\gamma$, where

$$a^\gamma = \exp\left(\frac{\mathrm{i}}{\hbar}\Omega_\gamma\right) \qquad \Omega_\gamma = \int_\gamma P(q,\hbar^2)\,\mathrm{d}q = \omega_\gamma + \mathrm{O}(\hbar^2). \tag{4}$$

The (formal) WKB expansion a^γ is called the *Voros multiplier* of the cycle γ (cf [22]), while $\omega_\gamma = \int_\gamma p\,\mathrm{d}q$ is the action integral over the cycle γ.

It is well known (cf [25] or [26], for instance) that these WKB expansions can be viewed as the asymptotics (with respect to $\hbar \to 0$) of analytic functions, at least locally in q when the WKB solutions are concerned. As a matter of fact, a stronger property holds: the WKB expansions enjoy the property of being *resurgent* (with respect to $1/\hbar \to \infty$)†. As explained in [21], this means that the WKB expansions are an *exact encoding* of analytic functions through the summation process, Borel-resummation or more generally some extensions of this Borel-resummation such as the lateral resummations (which coincide with the Borel-resummation in the case of Borel-summability) or median resummation.

The exact WKB method allows us to cover the (E,α)-space by various analytic charts in each of which exact analytic quantization conditions are given in terms of new 'model variables', related to the former (E,α) by (Borel or lateral) summable WKB expansions.

The necessary background is widely described in [20] in a 'do it by yourself' spirit, the theoretical point of view being more precisely discussed in [21].

4. Sketch of proofs

Searching for bound states amounts to finding those values E of (1) such that the subspace of wave solutions decaying at $-\infty$ coincides with the subspace of wave solutions decaying at $+\infty$. Let us translate this condition in terms of the representation (2) in a useful manner. We recall (cf [21]) that *Stokes lines* are defined in the same way as in Dingle [27]: hanging from turning points, these are level lines of $\mathrm{Re}\left(\int^q p(q')\,\mathrm{d}q'\right)$ in the q-complex plane (when the positive direction of summation is considered). In our case, the Stokes pattern has exactly five asymptotic directions at infinity, distributed according to the phases $\arg(q) = 3\pi/10 + 2k\pi/5$, $k = 0,\ldots,4$. Consequently, the property for a wave solution to decay at $-\infty$ (respectively, $+\infty$) is equivalent to the property for its (right or left) WKB symbol to be *recessive* (cf [20, 21]) along the Stokes line asymptotic to $\arg(q) = 11\pi/10$ (respectively, $-\pi/10$) at infinity.

4.1. First (critical) chart

First, we focus on what happens for positive real α, thus we set $\theta = 0$ in equation (2).

Looking for the quantization condition, some investigations show that it is convenient to localize $\widehat{E}$ near the relevant critical value $2/3\sqrt{3}$. For $\widehat{E} = 2/3\sqrt{3}$ the pattern of Stokes lines, drawn in figure 7, has a double turning point (at $q = -\mathrm{i}/\sqrt{3}$). This double turning is the crossing point when $\widehat{E} \to 2/3\sqrt{3}$ of a pair of simple turning points, symmetric with respect to the real axis when $\widehat{E}$ is real and greater than $2/3\sqrt{3}$. To this pair of coalescing simple turning

† For an introduction to the resurgence theory, see for instance [28].

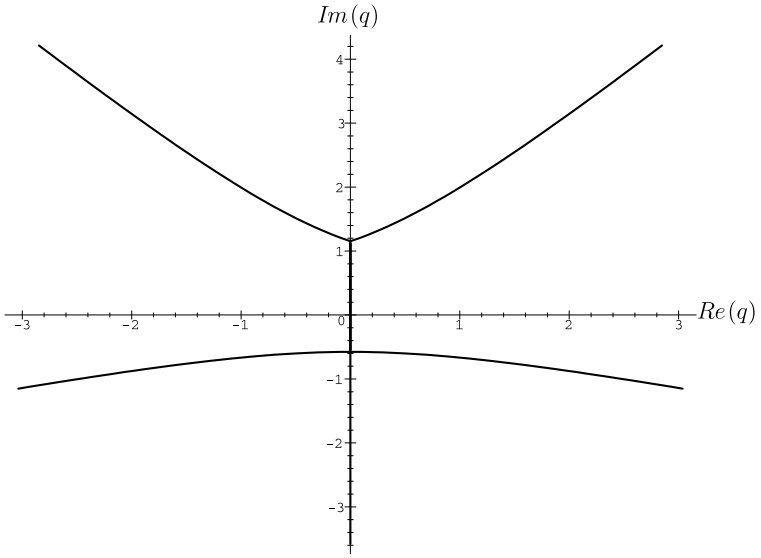

Figure 7. Critical Stokes pattern (real positive direction of summation).

points corresponds a cycle γ, like the one drawn in figure 6, called a *vanishing cycle*: this cycle, as well as the action integral ω_γ, vanishes when $\widehat{E} \to 2/3\sqrt{3}$.

The dependence of Ω_γ on $\widehat{E}$ is analytic (and even *regular*, in the sense of [21]) near the critical value $2/3\sqrt{3}$, allowing us to substitute $\widehat{E} = 2/3\sqrt{3} + \hbar E_r$ into Ω_γ. Defining

$$s(E_r, \hbar) = -\frac{1}{2} + \frac{\Omega_\gamma}{2\pi\hbar} | (\widehat{E} = 2/3\sqrt{3} + \hbar E_r)$$

we obtain the so-called (critical) *monodromy exponent* of the double turning point: it is a resurgent formal (WKB) series expansion, uniquely defined up to the orientation of the cycle γ. It is convenient for our purpose to choose this orientation so that $s = (3^{-1/4}E_r - 1)/2 + \mathrm{O}(\hbar)$ (an algorithm to obtain s is described in detail in [20]).

Using the same reasoning as in [20, section III.4], one easily obtains

$$\frac{1}{\Gamma(-s)} = 0 \tag{5}$$

for the secular equation. To see that equation (5) gives an *exact* quantization condition through resummation is a bit subtle: since the double turning point is tied to the simple turning point by a bounded Stokes line (figure 7), the monodromy exponent s is *not* Borel resummable, therefore the meaning of equation (5) may depend on which resummation (right, left, etc) is concerned. Nevertheless, as explained in [4], the *solutions* of equation (5) are the same *for all choices* (the same phenomenon as this one described in [20, section V.1.2] occurs here) so that:

- Solving equation (5) formally, which is also a Bohr–Sommerfeld-like equation $s = n$ for $n \in \mathbb{N}$, one obtains a power-series expansion†,

$$E_r^n = \sum_{k=0}^{\infty} E_{n,k} \hbar^k \tag{6}$$

† For this purpose, an algorithm can be found in [20].

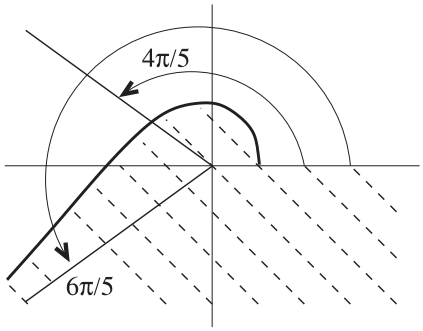

Figure 8. Domain of analyticity for the nth bound state in the α-complex plane for $\arg(\alpha) \geqslant 0$.

which is resurgent with respect to $1/\hbar$ (as a consequence of the implicit resurgence theorem [21]) and *Borel-resummable*, and whose Borel sum is precisely the exact solution of the secular equation (5);

- it follows from the $\mathcal{PT}$-invariance property and its very definition that s is *real*. Therefore, the reality property is true for the series expansion (6), and consequently, for its Borel-sum also.

Returning to the α variable, we obtain a slightly weaker version of claim 1:

Theorem 4.1 (See [4, 11, 14]). *There exists a domain of the form $\alpha > G(E)$, $E \in \mathbb{C}$, with G a positive continuous function of E, in which the spectral set of $\mathcal{H}_\alpha$ consists of a disjoint union of* real *analytic curves $E_n = E_n(\alpha)$, $n = 0, 1, \ldots$.*

In particular, the right-hand side of figure 1, which has been drawn by summing the Rayleigh–Schrödinger series to the least term, is valid for α large enough. More precise evaluations could be obtained by appealing to the hyperasymptotics [29–31].

$E_n(\alpha)$ have, however, a wider domain of analyticity. Arguments developed in [20, 21] and general nonsense in resurgence theory show that the Borel-transformed

$$\mathcal{B}(\hbar E_r^n)(\xi) = \sum_{k=0}^{\infty} E_{n,k} \frac{\xi^k}{\Gamma(k+1)}$$

of the series expansions $\hbar E_r^n(\hbar)$ extend analytically in the cut plane $\mathbb{C}\backslash]-\infty, -\frac{8}{5}3^{1/4}]$†, with a rate of growth at infinity less than an exponential function of order 1 inside all subsectors of this cut plane. Therefore, the Rayleigh–Schrödinger series (6) are resummable for an argument of direction of summation δ running on $]-\pi, +\pi[$. The Borel-sum

$$E_n(\alpha) = \alpha^{3/2} \left(\frac{2}{3\sqrt{3}} + \int_0^{\infty e^{i\delta}} e^{-\alpha^{5/4}\xi} \mathcal{B}(\hbar E_r^n)(\xi)\, d\xi \right)$$

is thus analytic in a sectorial neighbourhood of infinity S_n of aperture $]-6\pi/5, 6\pi/5[= \bigcup_{\delta \in\,]-\pi,+\pi[}]-2(\pi + 2\delta)/5, 2(\pi - 2\delta)/5[$ (see figure 8), the asymptotics at infinity being governed by the Rayleigh–Schrödinger series we started with: this is exactly claim 6. This property is also proved by independent means by Caliceti [14], while the Borel-summabilty of the Rayleigh–Schrödinger series was first proved in [11].

Remark. Furthermore, to enlarge the domain of analyticity, one is led to analyse the Stokes phenomena occurring for the directions of summation $\delta = \pm\pi$. When $\delta \lesssim -\pi$ for instance,

† $\pm\frac{8}{5}3^{1/4}\mathrm{i} = \pm 2\int_{-\mathrm{i}/\sqrt{3}}^{2\mathrm{i}/\sqrt{3}} p\, dq$ is the action period of the cycle running between the two turning points, with the sign depending on the orientation of the cycle.

it may be shown that the bound states $E_n(\alpha)$ can be encoded by a series of 'multi-instanton' expansions [20, 34]. However, their Borel-sums only converge in sectorial neighbourhoods of infinity of aperture $]-2(\pi + 2\delta)/5, 6\pi/5[$, so that nothing is gained. We return to this point later (section 4.3).

This first chart gives also claim 2 directly, apart from the asymptotic estimate for the general term of the Rayleigh–Schrödinger series for the nth energy level. This estimate (and even a hyperasymptotic series expansion), already announced in [4], can be derived (we leave it to the reader) from the resurgence structure of the monodromy exponent s, exactly in the same way as the one described in [20, section V.1.2] for the quartic oscillator (the rule played be the 'seen' singularity $-\frac{8}{5}3^{1/4}$, or 'adjacent' singularity in terms of hyperasymptotics, can be guessed in the given asymptotic estimate).

Note that there exists another way to compute the asymptotics for the coefficients of the Rayleigh–Schrödinger equation. For an even oscillator, it is known that part of the resurgence structure can be recovered from a dispersion formula, yielding the method developed in [32]. Under a natural assumption, Bender and Dunne show in [33] how such a dispersion relation can also be formulated for the $\mathcal{PT}$-symmetric cubic oscillator, and derive the asymptotic estimate of claim 2 (up to an easy rescaling).

We end this subsection with two remarks. From the fact that the analytic continuations of the bound states $E_n(\alpha)$ behave like $\frac{2}{3\sqrt{3}}\alpha^{3/2}$ when $|\alpha|$ goes at infinity with $\arg(\alpha) = \pm\pi$, one can infer that:

- the $E_n(\alpha)$ are multivalued functions: singularities can be expected for the analytic continuations;
- for each fixed n, $E_n(\alpha)$ cannot provide real eigenvalues for negative real α with $|\alpha|$ large enough.

4.2. Second (generic) chart

We now look for bound states for negative real α, and thus consider equation (2) with $\theta = \pi$ and $\widehat{E} > 0$. Applying the general methods developed in [20], one easily obtains

$$1 - 2\mathrm{e}^{U}\sin(\pi s) = 0 \tag{7}$$

for the quantization condition, where

$$\begin{aligned} U &= \frac{\mathrm{i}}{2\hbar}\int_{\gamma^\star+\gamma} P(q,\widehat{E},\hbar)\,\mathrm{d}q = x\left(u(\widehat{E}) + \mathrm{O}(x^{-2})\right) \\ s &= -\frac{1}{2} + \frac{1}{2\pi\hbar}\int_{\gamma^\star-\gamma} P(q,\widehat{E},\hbar)\,\mathrm{d}q = -\frac{1}{2} + \frac{x}{2\pi}\left(\omega(\widehat{E}) + \mathrm{O}(x^{-2})\right) \end{aligned} \tag{8}$$

with $x = 1/\hbar = (-\alpha)^{5/4}$.

The symmetric cycles γ and $\gamma^\star$, and their difference $\gamma^\star - \gamma$, have been represented in figure 9. Both U and s are resurgent Borel-resummable WKB expansions, and it follows from the $\mathcal{PT}$-symmetry property that:

Lemma 4.1. *The WKB expansions U and s are real.*

It may be checked that, for $\widehat{E}$ large enough, $u(\widehat{E})$ is a positive real function. Solving equation (7) formally thus means as a first step solving the equation $s = n$, where n is an integer: this is the generic analogue of the Bohr–Sommerfeld-like equation (5). This is, however, forgetting some small exponentials, which can be understood as 'multi-instanton' contributions [20, 34].

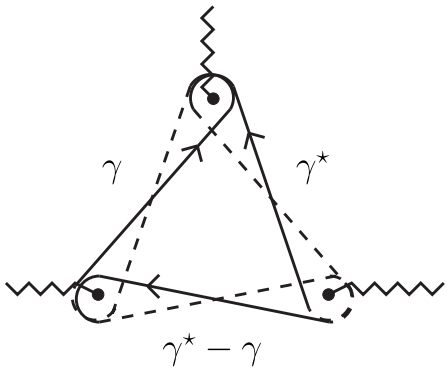

Figure 9. The cycles γ, $\gamma^\star$ and $\gamma^\star - \gamma$. The full circles are the three turning points.

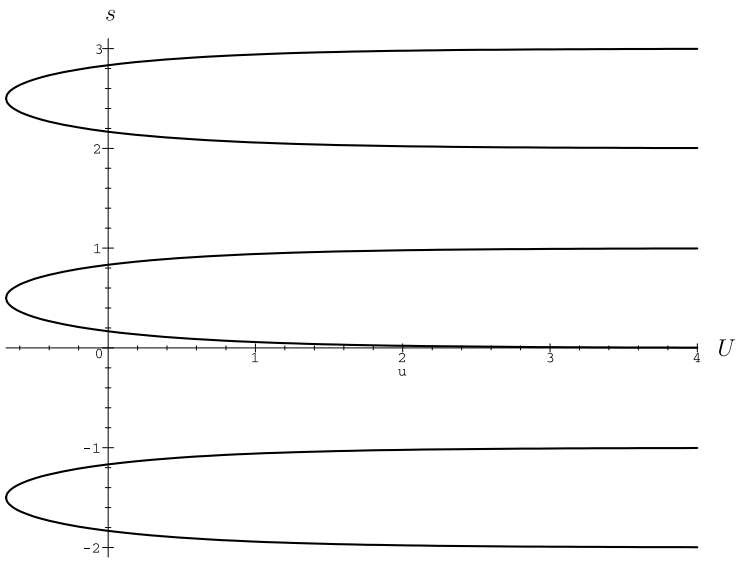

Figure 10. Secular equation (7): real solutions in the (U, s)-plane.

To gain a deeper understanding, one has to keep in mind that the quantization condition (7) is indeed an exact quantization through the Borel-summation process, with a main consequence: up to the *(resurgent, Borel-resummable) isomorphism*

$$(E, \alpha) \leftrightarrow (U, s)$$

between domains to be made precise later, equation (7) can be understood as a *model equation* in the sense of [19], i.e. an exact quantization condition in terms of the new variables (U, s), whose real solutions have been drawn in figure 10, revealing a branch point $U = -\ln(2)$ when s is understood as a function of U.

As a matter of fact, equation (7) describes a connected complex analytic curve in the $\mathbb{C}^2$-space of the variables (U, s), and figure 10 is just its real trace. We would now like to understand this analytic curve as a Riemann surface over the α-complex space (for $|\alpha|$ large enough).

The key remark to going further is the following lemma, which derives from general properties on elliptic functions (roughly, $\gamma^\star + \gamma$ and $\gamma^\star - \gamma$ are independent cycles, and

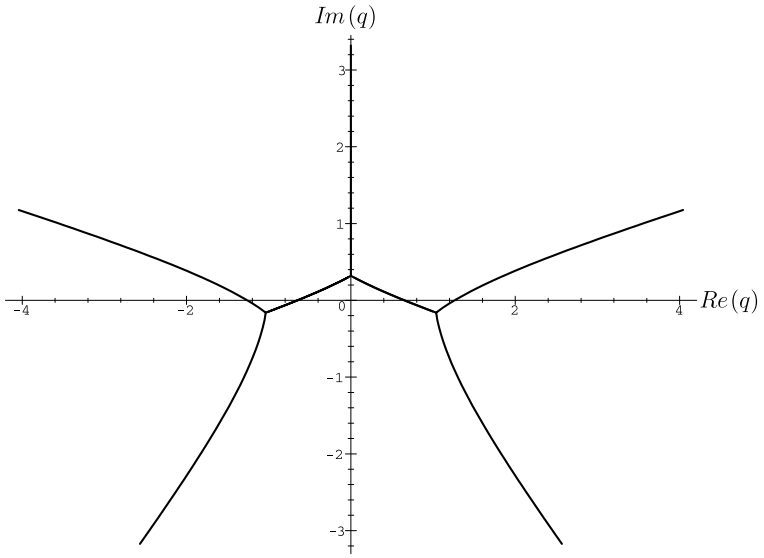

Figure 11. Anti-Stokes pattern for $\widehat{E} = \widehat{E}_0$.

the period lattice generated by $\int_{\gamma^\star+\gamma} \mathrm{d}q/p$ and $\int_{\gamma^\star-\gamma} \mathrm{d}q/p$ is non-degenerate, see [35] for instance).

Lemma 4.2. *There exists a unique* $\widehat{E} = \widehat{E}_0 \in [0, +\infty[$ *such that* $u(\widehat{E}) = 0$. *Moreover,* $\widehat{E}_0$ *is a simple zero of* $u(\widehat{E})$.

Remark. To such a value $\widehat{E}_0$ of $\widehat{E}$ corresponds a degenerate anti-Stokes pattern (i.e. when the direction of summation of argument $\pm\pi/2$ is considered) with a pair of symmetric bounded anti-Stokes lines (see figure 11). Computations give $\widehat{E}_0 = 0.352\,268\ldots$.

Along with lemma 4.2, it will be convenient to introduce some notation:

$$u_0' = \frac{\mathrm{d}u}{\mathrm{d}\widehat{E}}(\widehat{E}_0) = \tfrac{1}{2}\mathrm{i}\int_{\gamma^\star+\gamma} \frac{\mathrm{d}q}{2p}\bigg|\widehat{E} = \widehat{E}_0 \qquad \omega_0 = \omega(\widehat{E}_0)$$
$$\omega_0' = \frac{\mathrm{d}\omega}{\mathrm{d}\widehat{E}}(\widehat{E}_0) = \int_{\gamma^\star-\gamma} \frac{\mathrm{d}q}{2p}\bigg|\widehat{E} = \widehat{E}_0.$$

These constants $u_0', \omega_0, \omega_0'$ are real (by $\mathcal{PT}$-symmetry), and, in fact, positive: computations give $u_0' \sim 1.9548$, $\omega_0 \sim 2.571\,34$ and $\omega_0' \sim 3.1956$.

The idea is now to confine U in a bounded domain of the complex plane: both functions U and s are regular in $\widehat{E}$ near $\widehat{E}_0$, and we set $\widehat{E} - \widehat{E}_0 = E_r/x$ with E_r in a compact set $\mathcal{C}$ and we define

$$\mathcal{U}(x, E_r) = U(x, \widehat{E}) = u_0' E_r + h(x, E_r)$$
$$z(x, E_r) = s(x, \widehat{E}) = \frac{1}{2\pi}\left(x\omega_0 - \pi + \omega_0' E_r\right) + k(x, E_r)$$

where h and k are small resurgent functions in x with a regular dependence on E_r. The implicit resurgent function theorem [21] allows us to think of $(\mathcal{U}, z)$ as new variables, the inverse map

being given by

$$\begin{aligned} E_r(z,\mathcal{U}) &= \frac{\mathcal{U}}{u_0'} + H(z,\mathcal{U}) \\ x(z,\mathcal{U}) &= \frac{2\pi z}{\omega_0} + \frac{\pi}{\omega_0} - \frac{\omega_0'}{\omega_0 u_0'}\mathcal{U} + K(z,\mathcal{U}) \end{aligned} \tag{9}$$

where H and K are small resurgent functions in z with a regular dependence on $\mathcal{U}$ in a compact set $\mathcal{D}$.

This means localizing (E,α) in a neighbourhood of the analytic curve $E = \widehat{E}_0(-\alpha)^{3/2}$ for $|\alpha|$ large enough, and $\arg(-\alpha) \in]-2\pi/5, 2\pi/5[$ when the positive real direction of summation with respect to $1/\hbar = (-\alpha)^{5/4}$ is concerned. In such a range of (E,α), translating figure 10 yields the left-hand part of figure 1.

We now return to our quantization condition (7), which also reads as

$$\mathcal{U} = -\ln(2\sin(\pi z)) \bmod 2\mathrm{i}\pi \tag{10}$$

and analyse the singular locus. Differentiating (10), we obtain

$$\mathrm{d}z = -\frac{\tan(\pi z)}{\pi}\,\mathrm{d}\mathcal{U} \tag{11}$$

while (9) yields

$$\mathrm{d}x = \pi f_1(z,\mathcal{U})\,\mathrm{d}z - f_2(z,\mathcal{U})\,\mathrm{d}\mathcal{U} \tag{12}$$

with

$$\begin{aligned} f_1(z,\mathcal{U}) &= \frac{2}{\omega_0} + \mathrm{O}(z^{-2}) \\ f_2(z,\mathcal{U}) &= \frac{\omega_0'}{\omega_0 u_0'} + \mathrm{O}(z^{-1}). \end{aligned}$$

It follows from (11) and (12) that the tangent curve is thus given by

$$\mathrm{d}x = -(f_1(z,\mathcal{U})\tan(\pi z) + f_2(z,\mathcal{U}))\,\mathrm{d}\mathcal{U}. \tag{13}$$

As the resurgent function f_1 is invertible, we introduce the quotient

$$f(z,\mathcal{U}) = \frac{f_2}{f_1}(z,\mathcal{U}) = \frac{\omega_0'}{2u_0'} + \mathrm{O}(z^{-1})$$

and the function

$$\Phi(z,\mathcal{U}) = \arctan(f(z,\mathcal{U})) = \arctan\left(\frac{\omega_0'}{2u_0'}\right) + \varphi(z,\mathcal{U}) \tag{14}$$

with $\varphi(z,\mathcal{U})$ a small resurgent function. Formula (13) becomes

$$\mathrm{d}x = -\frac{f_1}{\cos(\pi z)\cos(\Phi)}\sin(\pi z + \Phi)\,\mathrm{d}\mathcal{U} \tag{15}$$

and yields (f_1 being invertible)

$$\tau = m \qquad m \in \mathbb{N} \qquad m \text{ large enough} \tag{16}_m$$

as a condition for the singular locus, where

$$\tau = z + \Phi/\pi = z + \frac{1}{\pi}\arctan\left(\frac{\omega_0'}{2u_0'}\right) + \frac{1}{\pi}\varphi(z,\mathcal{U}).$$

From the implicit resurgent function theorem, this last equality can be inverted, giving z as a resurgent function in τ with a regular dependence on $\mathcal{U} \in \mathcal{D}$:

$$z = \tau - \frac{1}{\pi} \arctan\left(\frac{\omega_0'}{2u_0'}\right) + \psi(\tau, \mathcal{U})$$

with ψ a small resurgent function. It then follows from $(16)_m$ that the branch points are solutions of the fixed-point problems

$$z = m - \frac{1}{\pi} \arctan\left(\frac{\omega_0'}{2u_0'}\right) + \psi(m, \mathcal{U}(z))$$

with $\mathcal{U}(z)$ given by (10). Remembering the condition $\mathcal{U} \in \mathcal{D}$, this yields

$$\begin{aligned} z_m^k &= m - \frac{1}{\pi} \arctan\left(\frac{\omega_0'}{2u_0'}\right) + \mathrm{O}(m^{-1}) \\ \mathcal{U}_m^k &= -\ln\left(\frac{2\omega_0'}{\sqrt{{\omega_0'}^2 + 4{u_0'}^2}}\right) - k\pi\mathrm{i} + \mathrm{O}(m^{-1}) \end{aligned} \qquad (17)_m^k$$

where ln denotes the usual determination of the logarithmic function and

$$(m, k) \in 2\mathbb{N} \times (2\mathbb{Z} + 1) \qquad \text{or} \qquad (m, k) \in (2\mathbb{N} + 1) \times 2\mathbb{Z} \qquad (18)$$

with m large enough and $|k| < Cste(\mathcal{D})$.

Translating these results in the x-plane by (9), we obtain the critical values

$$x_m^k = (2m+1)\frac{\pi}{\omega_0} - \frac{2}{\omega_0} \arctan\left(\frac{\omega_0'}{2u_0'}\right) + \frac{\omega_0'}{\omega_0 u_0'} \left\{ \ln\left(\frac{2\omega_0'}{\sqrt{{\omega_0'}^2 + 4{u_0'}^2}}\right) + k\pi\mathrm{i} \right\} + \mathrm{O}(m^{-1}) \qquad (19)_m^k$$

with (m, k) given by (18). It is straightforward to check on (15) that these singular points are square root branch points.

Riemann surface structure. We now describe the Riemann surface. On the z complex plane, we first consider an even, large, positive integer m. In order to think of $\ln(\sin(\pi z))$ as a univalued function, we begin to draw two cuts $]-\infty, m]$ and $[m+1, +\infty[$. In what follows, we choose the determination of the ln function so that $\ln(\sin(\pi z))$ is real for $z \in]m, m+1[$.

We now define the function $X(z)$ by substituting $\mathcal{U} = -\ln(2\sin(\pi z)) - k\pi\mathrm{i}$, $k \in 2\mathbb{Z}$ (formula (10)) into the function $x(z, \mathcal{U})$ of formula (9), and consider the 'steepest-descent' arcs of $\mathrm{Re}(X)$, hanging from the critical points z_{m+1}^k, z_m^{k+1} and z_m^{k-1}, whose image by X are horizontal half-lines (counted twice) in the x-plane, hanging from x_{m+1}^k, x_m^{k+1} and x_m^{k-1} respectively, and going along the positive real direction. These smooth arcs define the boundaries of a deformed vertical cut strip which will be called the (m, k) *z-strip* (see figure 12). This strip maps conformally onto the horizontal (m, k) *x-strip* of the x-complex plane, as shown in figure 13.

However, we have to take into account that everything has been done for $\mathcal{U}$ in a compact set $\mathcal{D}$. This implies considering z (respectively, x) only in a compact set deprived of an open neighbourhood of the logarithmic singularity $z = m$ (respectively, in a compact set); see figures 12 and 13.

Starting from the (m, k) z-strip and turning around the logarithmic singularity m (along the path δ of figure 12, for instance) amounts to adding or subtracting an even integer to k. Through the conformal mapping, this means that each (m, k) x-strip can be glued with its

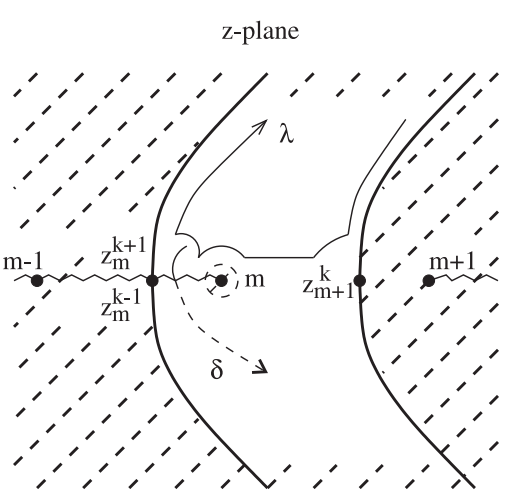

Figure 12. The (m, k) z-strip for even m.

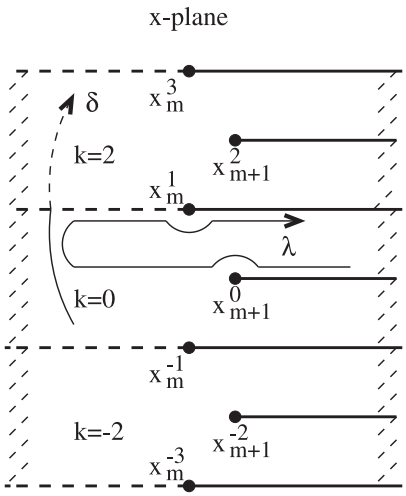

Figure 13. The (m, k) x-strip for even m and $k = -2, 0, 2$. The path λ (respectively, δ) drawn in figure 11 with $k = 0$ is mapped onto the path λ (respectively, δ) in this figure. Forgetting the horizontal dotted lines, one obtains the mth sheet.

neighbouring $(m, k \pm 2)$ x-strip, to give what will be called the *mth sheet* (see figure 13). One defines the sheets for odd m in a similar way.

Starting from the mth sheet, m even, and crossing the cut issued from the branch point x_{m+1}^k (respectively, $x_m^{k\pm1}$), one merges into the $(m+1)$th sheet (respectively, $(m-1)$th sheet). The proof is just an easy translation from the z-plane to the x-plane. For the same reason, if m is odd, the cut issued from the branch point x_m^k (respectively, $x_{m+1}^{k\pm1}$) is the borderline between the mth and the $(m-1)$th sheet (respectively, $(m+1)$th sheet).

Translating these results in terms of the α variable, we thus obtain:

Theorem 4.2. *For every $m_o \in \mathbb{N}$ large enough, there exists a bounded neighbourhood $\mathcal{C}(m_o)$ of $-\left((2m_o+1)\frac{\pi}{\omega_0}\right)^{4/5}$ in the α-complex plane such that the quantization condition, restricted to a neighbourhood of the analytic curve $E = \widehat{E}_0(-\alpha)^{3/2}$, describes a connected Riemann surface over $\mathcal{C}(m_o)$ with only square root branch points at $\alpha_m^k = -(x_m^{k\,4/5})$,*

$$x_m^k = (2m+1)\frac{\pi}{\omega_0} - \frac{2}{\omega_0}\arctan\left(\frac{\omega_0'}{2u_0'}\right) + \frac{\omega_0'}{\omega_0 u_0'}\left\{\ln\left(\frac{2\omega_0'}{\sqrt{\omega_0'^{\,2}+4u_0'^{\,2}}}\right) + k\pi\mathrm{i}\right\} + \mathrm{O}(m^{-1})$$

with $(m, k) \in 2\mathbb{N} \times (2\mathbb{Z}+1)$ or $(m, k) \in (2\mathbb{N}+1) \times 2\mathbb{Z}$.

Theorem 4.2 gives partly the westbound description of section 2: each mth sheet of the x-plane is conformally mapped onto an mth sheet in the α-plane as exemplified in figures 2 and 3, where a *real* eigenvalue E_m^W can be defined. The relationship between the E_m^Ws through analytic continuations are in perfect agreement with our claim 4 and its comments, apart from the fact that our results are essentially local and, consequently at this stage, we have no reason to interpret the mth west bound state $E_m^W(\alpha)$ as analytic continuations of the mth bound states $E_m(\alpha)$ obtained from the first chart. To complete the drawing one thus needs to resort to other charts.

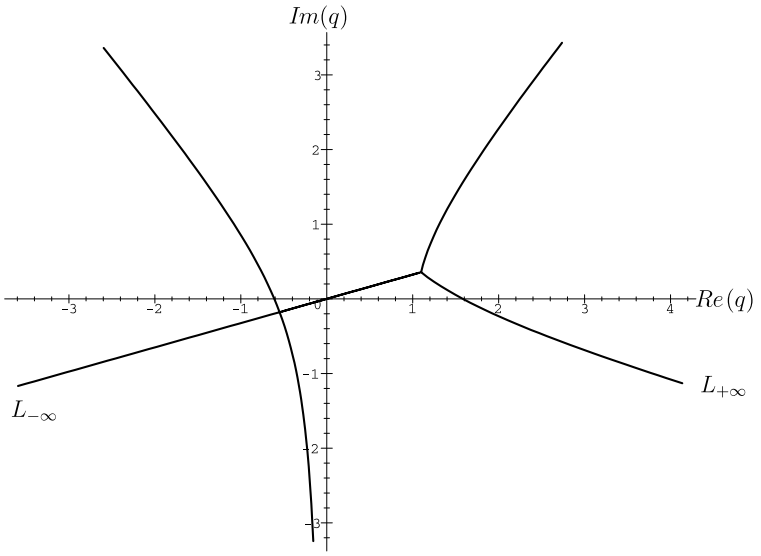

Figure 14. Critical Stokes pattern for $\varepsilon = -1$ (real positive direction of summation).

4.3. Third (critical) chart

We return to equation (2) and now set $\theta = \varepsilon 4\pi/5$, $\varepsilon = \pm$, which means centring the phase of α on $\varepsilon 4\pi/5$. Remembering from claim 6 (or chart 1) that the analytic continuations of each $E_n(\alpha)$ are asymptotic to $\frac{2}{3\sqrt{3}}\alpha^{3/2}$ at infinity, we start by considering the critical Stokes pattern for $\widehat{E} = \frac{2}{3\sqrt{3}}\exp(\varepsilon 6\mathrm{i}\pi/5) + \mathrm{O}(\hbar)$, as drawn in figure 14. It is interesting to note that, up to a small rotation, figure 14 is exactly the Stokes pattern of a cubic barrier when one localizes near the bottom of the well. Indeed, performing the change of variables

$$Q = \mathrm{e}^{\varepsilon \mathrm{i}\pi/10} q \qquad \widetilde{E} = \mathrm{e}^{-\varepsilon \mathrm{i}\pi/5}\widehat{E} \tag{20}$$

in the Schrödinger equation (2), one obtains

$$-\hbar^2 \frac{\mathrm{d}^2}{\mathrm{d}Q^2}\Phi + \varepsilon(Q^3 - Q)\Phi = \widetilde{E}\Phi \tag{21}$$

with $\widetilde{E} = -\frac{2}{3\sqrt{3}} + \mathrm{O}(\hbar)$. At first sight, such a result may appear confusing: to equation (21) corresponds the Hamiltonian $p^2 + \varepsilon(Q^3 - Q)$, which is *not* a self-adjoint operator (when defined on its maximal domain); it admits infinitely many self-adjoint extensions, each one with a pure point spectrum, thus leading to the non-uniqueness of the quantum dynamics (see [11, 36])!

Fortunately, as our change of space variable (20) now induces a rotation in the complex domain, one has to take care of the fact that considering solutions of (1) in the Hilbert space $L^2(\mathbb{R})$ *does not* mean considering solutions $\Phi \in L^2(\mathbb{R})$ for equation (21).

- The $\varepsilon = -1$ case. The L^2 solutions of equation (2) can be characterized by their exponential decay at infinity along the two Stokes lines $L_{-\infty}$ and $L_{+\infty}$ drawn in figure 14. Translating this requirement of equation (21) means looking for exponentially decaying functions at infinity along the two Stokes lines $L_{-\infty}$ and $L_{+\infty}$ drawn in figure 15. This amounts to finding the (complex) values of the energies $\widetilde{E}$ such that an incident wave

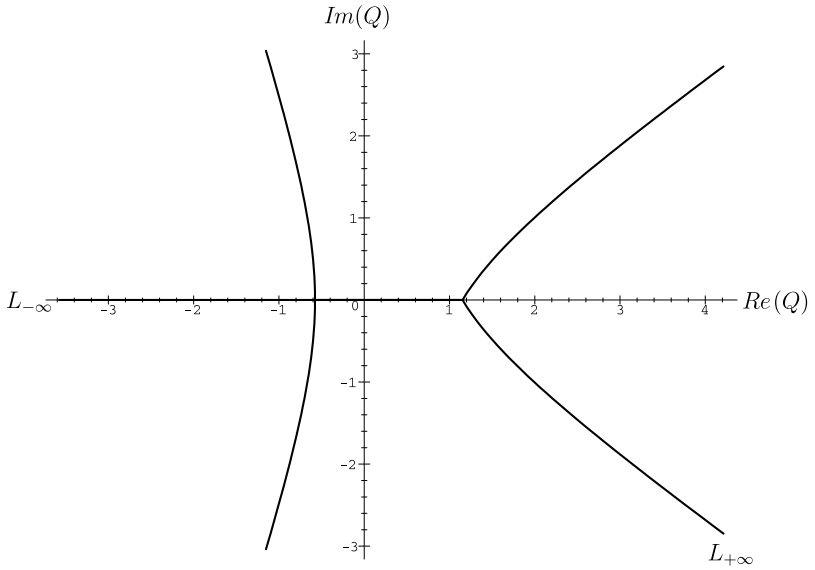

Figure 15. As for figure 14, but with equation (21).

coming from the right has a vanishing reflected component: this is exactly looking for the *resonance* values (compare with [11, 14]).

- The $\varepsilon = +1$ case. Since this case can be derived from the previous $\varepsilon = -1$ case by complex conjugation in α, here we are thus looking for the *complex conjugate of the resonance* values.

The resonance values of a cubic barrier near the bottom of the well have already been studied in [20] from the viewpoint of an exact semiclassical analysis. Translating (part of) these results here, one deduces from the existence of a bounded Stokes line in figure 14 that the eigenvalues $E_n(\alpha)$ cease to be the Borel sums of their Rayleigh–Schrödinger series expansions for the range of α considered here ($\alpha \in]-6\pi/5, -2\pi/5[$ or $]2\pi/5, 6\pi/5[$, depending on ε), as announced in the remark of section 4.1.

The properties of the resonance values for a cubic barrier near the top of the well are less known but, from what we know for a double well for instance (cf [37, 38]), one can guess an interesting microlocal concentration (in the semiclassical limit) for the resonances values near the top of the cubic barrier. Moreover, it has been shown in [19] that this phenomenon for a double well was nothing but the real trace of an exponentially close singular structure in the complex domain.

Thus, being interested here in the singular behaviour of the spectrum, we shall localize our study near the top of the cubic barrier, which means considering large quantum numbers for large $|\alpha|$. We thus set

$$\widetilde{E} = \frac{2}{3\sqrt{3}} + \hbar E_r \qquad \left(\text{so that} \quad E \sim -\frac{2}{3\sqrt{3}}\alpha^{3/2}\right). \tag{22}$$

Choosing $\varepsilon = -1$ (say) in (21), arguments based on [20] again show that the (exact) quantization condition simply reads

$$1 + a = 0 \tag{23}$$

where a is a 'critical Voros multiplier' associated with the (connection) oscillator cycle. It is a Borel-resummable WKB expansion whose computation can be done to all orders (cf [21]), yielding

$$a = \frac{\sqrt{2\pi}\mathrm{e}^{U/4}}{\Gamma\left(\frac{1}{2}+\mathrm{i}U/2\pi\right)}\left(\frac{c}{\hbar}\right)^{\mathrm{i}U/2\pi}\mathrm{e}^{\mathrm{i}\omega/\hbar}\mathrm{e}^{-\mathrm{i}D}.$$

The constant $\omega = \frac{8}{5}(3^{1/4})$ is the action integral over the oscillator cycle, while $c = 96(3^{1/4}) = 60\omega$ is the so-called critical action multiplier [20, 21]. The real WKB series expansion

$$U(E_r,\hbar) = 3^{1/4}2\pi\left(\tfrac{1}{5}\sqrt{3}\,E_r + \left(\tfrac{7}{576}\sqrt{3} - \tfrac{5}{192}E_r^2\right)\hbar + \left(-\tfrac{455}{18\,432}E_r + \tfrac{385}{55\,926}\sqrt{3}E_r^3\right)\hbar^2\right) + \mathrm{O}(\hbar^3)$$

is related to the (critical) monodromy exponent s of the double turning point through the equality $s + \frac{1}{2} = \mathrm{i}U/2\pi$, and D is a small real WKB series expansion:

$$D(E_r,\hbar) = 3^{1/4}\left(\left(\tfrac{72}{1152}\sqrt{3} - \tfrac{47}{384}E_r^2\right)\hbar + \left(-\tfrac{15\,911}{110\,592}E_r + \tfrac{11\,947}{331\,776}\sqrt{3}E_r^3\right)\hbar^2\right) + \mathrm{O}(\hbar^3).$$

From now on, our analysis will follow the spirit of [19], allowing us to be rather sketchy.

Instead of working with the variables $(E_r, \hbar)$, we study our quantization condition in terms of variables (U, X), where X is the 'model variable' defined implicitly by

$$a = \frac{\sqrt{2\pi}\mathrm{e}^{U/4}}{\Gamma\left(\frac{1}{2}+\mathrm{i}U/2\pi\right)}X^{\mathrm{i}U/2\pi}\mathrm{e}^{\mathrm{i}X}$$

and whose existence is guaranteed by the resurgent implicit theorem [21]:

$$X(U,\hbar) = \lambda + \frac{U}{2\pi}\ln 60 - \left(\frac{24}{205} + \frac{U^2}{\pi^2}\left(\frac{47}{80} + \frac{\ln 60}{4}\right)\right)\lambda^{-1} + \mathrm{O}(\lambda^{-2}) \qquad (24)$$

with

$$\lambda = \frac{\omega}{\hbar}.$$

One can thus write the quantization condition (23) in the form

$$\exp(\mathrm{i}\theta) = -\frac{\Gamma\left(\frac{1}{2}+\mathrm{i}U/2\pi\right)}{\sqrt{2\pi}\mathrm{e}^{U/4}} \qquad (25)$$

where

$$\theta = X + \frac{U}{2\pi}\ln(X).$$

The secular equation (25) gives immediately the nth bound state in terms of an analytic relation between X and U:

$$X + \frac{U}{2\pi}\ln(X) = (2n+1)\pi + \mathrm{i}\tfrac{1}{4}U - \tfrac{1}{2}\mathrm{i}\ln\frac{\Gamma^2\left(\frac{1}{2}+\mathrm{i}U/2\pi\right)}{2\pi}. \qquad (26)_n$$

Noting that $\Gamma(\frac{1}{2}+\mathrm{i}U/2\pi)$ is a meromorphic function with a lattice of *simple* poles located at

$$u_k = 2\mathrm{i}\pi\left(k - \tfrac{1}{2}\right) \qquad k \in \mathbb{N}\backslash\{0\}$$

running clockwise around one of these poles results in adding 1 to the quantum number n in equation $(26)_n$. Thus, the analytic relations $(26)_n$ actually describe different branches of a single complex curve in the space $\mathbb{C}^2$ of the variables (X, U), which will be seen as a Riemann surface $\mathcal{S}$ over the X-complex plane.

We now want to analyse, for $|X|$ large enough and $|\arg(X)| < \pi/2$, this Riemann surface $\mathcal{S}$. Differentiating equation $(26)_n$ yields

$$\left(1 + \frac{U}{2\pi X}\right) \mathrm{d}X = \left(-\frac{\ln X}{2\pi} + \frac{\mathrm{i}}{4} + \frac{1}{2\pi}\Psi\left(\frac{1}{2} + \frac{\mathrm{i}U}{2\pi}\right)\right) \mathrm{d}U \tag{27}$$

where $\Psi(z) = \frac{\mathrm{d}}{\mathrm{d}z} \ln \Gamma(z)$ is the digamma function. Adding the condition $\mathrm{d}X = 0$ to this equation (27), we obtain

$$\Psi\left(\frac{1}{2} + \frac{\mathrm{i}U}{2\pi}\right) = \ln X - \tfrac{1}{2}\mathrm{i}\pi \tag{28}$$

for the ramification condition.

For $\mathrm{Re}(\ln X) \gg 1$, equation (28) implies that $\frac{1}{2} + \mathrm{i}U/2\pi$ necessary stands in a neighbourhood of a pole of the digamma function, i.e. U near $u_k = 2\mathrm{i}\pi(k - \frac{1}{2})$, $k \in \mathbb{N}\backslash\{0\}$. Precisely, solving (28) yields a sequence $(U_k(\ln X))_{k\in\mathbb{N}\backslash\{0\}}$ of holomorphic functions of $\ln X$,

$$U_k(\ln X) = u_k + \frac{2\mathrm{i}\pi}{\ln X} + \cdots \in \mathbb{C}\{\ln X\}. \tag{29}_k$$

Substituting $(29)_k$ in $(26)6n$, one finally obtains the fixed-point problem

$$X = F^n_{\pm k}(X) \tag{30}^n_{\pm k}$$

with

$$F^n_{\pm k}(X) = (2n \pm k + 1)\,\pi - \frac{U_k(\ln X)}{2\pi} \ln(X) + \mathrm{i}\frac{U_k(\ln X)}{4} - \tfrac{1}{2}\mathrm{i} \ln \frac{\Gamma^2\,(1/2 + \mathrm{i}U_k(\ln X)/2\pi)}{2\pi}$$

where n is an integer, and the determination of the logarithm is chosen to be real along the positive real axis.

It follows from (28) that

$$\frac{\mathrm{d}}{\mathrm{d}X} F^n_{\pm k}(X) = -\frac{U_k(\ln(X))}{2\pi X}.$$

For $|X| \geqslant C$ with C chosen large enough, one can assume that $U_k(\ln(X))$ (given by $(29)_k$) satisfies

$$|U_k - u_k| \leqslant r_k < \pi \tag{31}$$

hence $|U_k| < 2\pi k$, and we obtain

$$\left|\frac{\mathrm{d}}{\mathrm{d}X} F^n_{\pm k}(X)\right| < \frac{k}{C} < 1$$

under the condition $0 < k < C$, i.e. $F^n_{\pm k}$ is a contractive map. To ensure that our fixed-point problem $(30)^n_{\pm k}$ has a unique solution, it remains to check that the domain is stable under $F^n_{\pm k}$. Introducing $Y = \ln(X)$, our domain is now defined by

$$\mathrm{Re}(Y) > \ln(C) \qquad \text{and} \qquad -\pi/2 < \mathrm{Im}(Y) < \pi/2$$

and the fixed-point problem becomes

$$Y = \ln(G^n_{\pm k}(Y))$$

with

$$G^n_{\pm k}(Y) = (2n \pm k + 1)\,\pi - \frac{U_k(Y)}{2\pi} Y + \mathrm{i}\frac{U_k(Y)}{4} - \tfrac{1}{2}\mathrm{i} \ln \frac{\Gamma^2\left(\frac{1}{2} + \mathrm{i}U_k(Y)/2\pi\right)}{2\pi}.$$

With the range of U_k considered here, the ln term on the right-hand side of our last equality can be written as

$$-\tfrac{1}{2}\mathrm{i}\ln\frac{\Gamma^2\left(\frac{1}{2}+\mathrm{i}U_k(Y)/2\pi\right)}{2\pi} = -\mathrm{i}\ln(Y) + B_k(Y)$$

where B_k is a bounded function. Furthermore, using (31), we obtain

$$G^n_{\pm k}(Y) = \left(2(n \pm \tfrac{1}{2}k) - \tfrac{1}{2}k + \tfrac{5}{4}\right)\pi - \mathrm{i}(k-\tfrac{1}{2})Y - \mathrm{i}\ln(Y) + D_k(Y)$$

with D_k a bounded function, say $|D_k| \leqslant d_k$. It is now clear that a necessary condition for the domain to be stable is to impose

$$-\pi/2 < \mathrm{Im}(Y) < 0$$

which corresponds to the condition

$$-\pi/2 < \arg(X) \leqslant 0$$

for the variable X. Note here that this result is in agreement with our claim 5 and its consequence in the X-variable: no singularities were expected in the domain $0 < \arg(X) < \pi/2$ and $|X|$ large enough.

One easily checks that the demand $|G^n_{\pm k}(Y)| > C$ (hence $\mathrm{Re}(\ln(G^n_{\pm k}(Y))) > \ln(C)$) will be satisfied if

$$\left(2n \pm k - k + \frac{3}{2}\right)\pi > C + \frac{\pi}{2\ln(C)} + d_k. \tag{32}$$

Under this condition, we can apply the fixed-point theorem to $(30)^n_{\pm k}$ which provides a unique branch point of $U(X)$, denoted by $X^{n\pm k/2}_{k/2}$, with the value $U^{n\pm k/2}_{k/2}$ given by $(29)_k$. The square root nature of the branch point obviously follows from (28). In summary:

Theorem 4.3. *For any positive integer K, there exists a constant C_K such that the quantization condition describes a connected Riemann surface $\mathcal{S}$ over the domain $\{|X| > C_K,\ -\pi/2 < \arg(X) \leqslant 0\}$, with only square root branch points at $(X^{n\pm k/2}_{k/2}, U^{n\pm k/2}_{k/2})$ with $k = 1, 2, \ldots, K$ and n any positive integer larger than a constant depending on k. Moreover, for fixed k,*

$$\mathrm{Re}(X^{n\pm k/2}_{k/2}) = \left(2(n \pm \tfrac{1}{2}k) - \tfrac{1}{2}k + \tfrac{5}{4}\right)\pi + \mathrm{O}\left(\frac{1}{\ln n}\right)$$

$$\mathrm{Im}(X^{n\pm k/2}_{k/2}) = -(k-\tfrac{1}{2})\ln n - \ln(\ln n) + \mathrm{O}(1)$$

(corresponding to $U = U^{n\pm k/2}_{k/2} \sim u_k$) asymptotically with $n \to +\infty$ ($n \in \mathbb{N}$).

Addendum. Our theoretical result (33) shows that the fixed-point problem $(30)^n_{\pm k}$ converges when $n - k$ is positive and large enough, and, consequently, the quantum number n is a (large enough) positive integer as it might be. Numerical evidence shows that our iteration scheme $(30)^n_{\pm k}$ converges as soon as $n - k \geqslant 0$.

In order to understand the sheet structure of our Riemann surface, we return to the quantization condition $(26)_n$ for a given quantum number $n \in \mathbb{N}$ large enough. Starting with a U close to zero, let us climb up the imaginary U-axis along paths avoiding the singularities u_k ($k = 1, 2, \ldots$) by small half-circular detours as shown in figure 16, (top). Their conformal images (by $(26)_n$) are drawn in figure 16, (bottom) (please ignore the vertical half-lines).

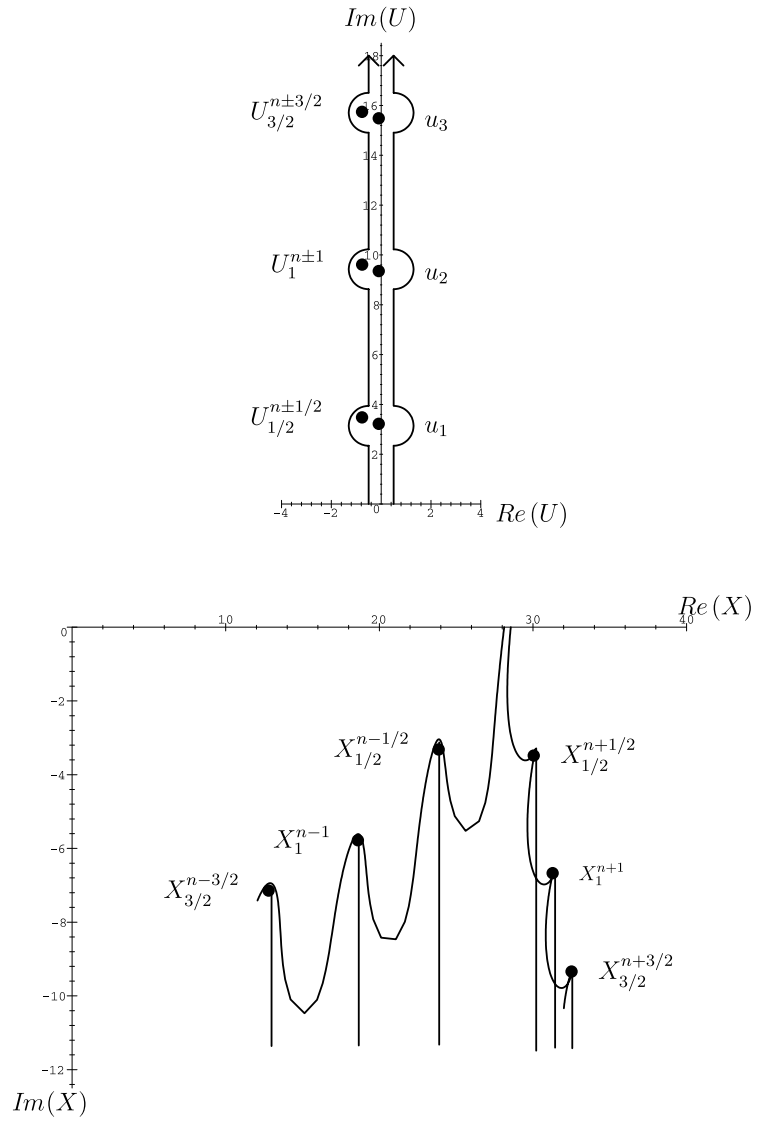

Figure 16. The right (respectively, left) path in the U-plane (top) is conformally mapped onto the left (respectively, right) path in the X-plane (bottom) through the analytic relations $(26)_n$ (here $n = 4$).

When U approaches the singularity u_k, $\mathrm{Im}(X)$ goes to $-\infty$, while U turning around the quadratic point $U_{k/2}^{n\pm k/2}$ (with $\pm = -$ for the right-hand path and $\pm = +$ for the left-hand path), close to u_k when n is large, makes X turn around the corresponding branch point $X_{k/2}^{n\pm k/2}$.

Each of the vertical half-lines $L_{k/2}^{n\pm k/2}$ drawn in figure 16 (bottom), hanging from $X_{k/2}^{n\pm k/2}$, which will play the role of cuts, is the image (counted twice) of two smooth arcs, close to the imaginary U-axis, running from $U_{k/2}^{n\pm k/2}$ to u_k and u_{k+1}, respectively. We call the resulting cut plane the *nth sheet*, on which a univalued function $U_n(X)$ can be defined as the nth determination of the multivalued function $U(X)$.

Noting that crossing (u_k, u_{k+1}) from left to right increases the quantum number n by k in $(26)_n$, one sees that $L_{k/2}^{n\pm k/2}$ is a common frontier between the nth sheet and the $(n \pm k)$th sheet (which corresponds to adding and subtracting the superscript and subscript of $X_{k/2}^{n\pm k/2}$): our knowledge of the Riemann surface $\mathcal{S}$ is now complete.

Nevertheless, translating our previous result in terms of the (α, E) variable requires a slight modification as in [19], section 3.3. Since the model variable X actually depends on U (cf (24)), this results in a small distortion in the projection. Precisely to obtain the branch points of the projection on the complex α-plane, one should rewrite $\mathrm{d}X$ in terms of $\mathrm{d}\lambda$ and $\mathrm{d}U$ in equation (27), thus obtaining

$$\Psi\left(\frac{1}{2}+\frac{\mathrm{i}U}{2\pi}\right)=\ln X-\frac{\mathrm{i}\pi}{2}-\ln 60+\frac{U}{\pi}\left(\frac{47}{20}+\frac{\ln 60}{2}\right)X^{-1}+\mathrm{O}(X^{-2}) \quad (28')$$

in place of (28) for the ramification condition.

This modification does not change our concluding theorem 4.3 and its comments. From the numerical point of view, the effect is small indeed, even for small values of the quantum number n. All computations have been done with this modified equation (28′) (and $(30)_{\pm k}^{m}$ modified accordingly).

Translating each nth sheet (respectively, each determination $U_n(X)$) in the α-plane yields what we can call the 'north-west' nth sheet (respectively, the nth 'north-west' spectral function $E_n^{NW}(\alpha)$). From the numerical side, this requires:

- to compute $\lambda = \omega(\mathrm{e}^{4\mathrm{i}\pi/5}\alpha)^{5/4}$ as a resurgent (resummable) series expansion in terms of our model variable X. This can be done algorithmically from its definition (24):

$$\lambda=X-\frac{U}{2\pi}\ln 60+\left(\frac{24}{205}+\frac{U^2}{\pi^2}\left(\frac{47}{80}+\frac{\ln 60}{4}\right)\right)X^{-1}+\mathrm{O}(X^{-2}) \quad (33)$$

- to compute its Borel-sum. We have done it rather crudely, just using the first few terms of its asymptotics (33). For a more precise numerical resummation, one may appeal to the hyperasymptotic theory as detailed in [29–31].

The symmetric 'south-west' nth sheet (respectively, the nth 'south-west' spectral function $E_n^{SW}(\alpha)$), deduced from its 'north-west' version by complex conjugation, is exactly what is drawn in figure 5 (with $n = 3$): each singular point $X_{k/2}^{n\pm k/2}$ being a common branch point for $U_n(X)$ and $U_{n\pm k}(X)$, its corresponding point $\alpha_{k/2}^{n\pm k/2}$ is thus a common branch point for $E_n^{SW}(\alpha)$ and $E_{n\pm k}^{SW}(\alpha)$: the branch point $\alpha_{k/2}^{n-k/2}$ (respectively, $\alpha_{k/2}^{n+k/2}$) is much conveniently denoted by the bracket $[n, n-k]$ (respectively, $[n+k, n]$)) in figure 5.

Drawing all the branch points $\alpha_{k/2}^{n\pm k/2}$ with $n \in \mathbb{N}$, $k \in \mathbb{N}\backslash\{0\}$ and $n - k \geqslant 0$, yields figure 4. It may be checked numerically that the sequence of *real* branch points is exactly described by the sequence $\alpha_{(n+1)/2}^{n+(n+1)/2}$, $n \in \mathbb{N}$ (or equivalently by the brackets $[2n+1, n]$ with the convention of figure 5).

To conclude this section, we summarize the main ideas we used for deriving theorem 4.3. We started with the fact that any bound state $E_n(\alpha)$ obtained from the first chart can be analytically continued in a convenient sectorial neighbourhood of infinity centred on $\arg(\alpha) = \pm 4\pi/5$, and behaves like $\frac{2}{3\sqrt{3}}\alpha^{3/2}$ when $|\alpha|$ goes to infinity in the sector. To obtain information concerning the singularities for large $|\alpha|$, it was thus necessary to consider large enough quantum numbers n. Comparisons with resonance values of the real cubic oscillator led us to choose this range of (n, α) such that $n = \mathrm{O}(|\alpha|^{5/4})$ (cf theorem 4.3 and (33)), while $E_n(\alpha) \sim -\frac{2}{3\sqrt{3}}\alpha^{3/2}$.

5. Conclusion

Our set of charts is now (almost) complete, giving convenient information over the whole α-plane, except of course for the neighbourhood of the origin which are beyond the scope of our tools.

To obtain a complete portrait of the global ramification, all we have to do is to match together this set of information. We saw from our first chart that the eigenvalues $E_n(\alpha)$ can be analytically continued in a full sector S_n of aperture $|\arg(\alpha)| < 6\pi/5$ where $E_n(\alpha) \sim \frac{2}{3\sqrt{3}}\alpha^{3/2}$ when $|\alpha| \to \infty$. The third chart completes this first approach. From theorem 4.3 and the remark ending section 4.3, we deduce that the $E_n(\alpha)$s extend as a sole multivalued analytic function, with a quasi-lattice of singularities in a subsector of $\arg(\alpha) \in]4\pi/5, 6\pi/5[\bmod(2\pi)$. Our theorem 4.3 translates into a concrete qualitative and quantitative insight for the branch point structure (south-west or north-west sheets), which is consistent with our comments following claim 6, up to the following restriction: considering for instance the south-west description, one should keep in mind that, for a given quantum number n, theorem 4.3 provides valuable asymptotic information concerning *a priori* only a finite set of singularities $\alpha_{k/2}^{n\pm k/2}$, near which $E_n(\alpha) \sim -\frac{2}{3\sqrt{3}}\alpha^{3/2}$, corresponding to a finite number of integers k. The fact that the set of branch points $\alpha_{k/2}^{n+k/2}$ cannot accumulate but indeed goes to infinity in the direction of argument $6\pi/5$ (where $E_n(\alpha) \sim \frac{2}{3\sqrt{3}}\alpha^{3/2}$) for any n-south-west sheet, which means letting k go to infinity, thus has no theoretical support but only a numerical one.

Starting from the collection of south-west and north-west n-sheets ($n \in \mathbb{N}$), one can deduce the equivalent but simpler west representation, as exemplified in figures 2 and 3, which is a more suitable representation to understand the analytic continuations along the real axis for instance. To compare with what we know from the second chart (theorem 4.2), we consider the nth south-westbound description (figure 5) and straighten out the cuts to put them almost horizontal, asymptotic at infinity to the negative real axis (the distance between the cuts and the real axis behaving like $O(1/|\alpha|)$ when $|\alpha| \to \infty$, for instance). Along the deformation, some of the branch points appear (respectively, disappear) from (respectively, into) other sheets. A little thought (using our knowledge on how the different south-west and north-west sheets are connected) yields the following conclusion; the nth west sheet has a set of $2n + 1$ cuts: n of them, hanging from $\alpha_{k/2}^{n-k/2}$, $k = 1, \ldots, [(n + 1)/2]$ (where $[a]$ denotes the integer part of a) and their complex conjugates, are common boundary cuts with the $(n - 1)$th west sheet, while $n + 1$ of these cuts, hanging from $\alpha_{k/2}^{n+1-k/2}$, $k = 1, \ldots, 1 + [n/2]$ and their complex conjugates, are common boundary cuts with the $(n + 1)$th west sheet. This qualitative result is in complete agreement with what we obtained from the second chart with, again, a warning: the above reasoning is partly based on the addendum following theorem 4.3; we thus did not take care concerning the theoretical prescriptions on the quantum numbers n and the labels k. As a matter of fact, the 'median' second chart gives rigorous information in a neighbourhood of the singularity $\alpha_{k/2}^{n-k/2}$ with $k = [(n+1)/2]$ near the negative real axis (where $E_n(\alpha) \sim \widehat{E}_0(-\alpha)^{3/2}$), hence for a label k half as large as the quantum number n. Consequently, even if numerical computations give us good reason to think that our charts two and three overlap, this has not been proved.

From a rigorous point of view, and apart from the above technicalities, the very nature of our (exact semiclassical) asymptotic tools prevents us from giving the global ramification in its full extent, our collection of (west, south-west or north-west) n-sheets being only valid for α large enough (and E large enough accordingly). For instance the broken curves plotted in the central part of figure 1 are nothing but *bid interpolating* curves between what we know from the right-hand part (first chart) and left-hand part (second and third chart) of the picture! It thus

remains an 'unknown zone' (as called in [19]), corresponding to an open set $|E| = o(|\alpha|^{3/2})$ in $\mathbb{C}^2$, where other methods should be apply. One of them could be the new quantization approach developed by Voros [39, 40].

Nevertheless, the good convergence of our numerical schemes, even for small $|\alpha|$, as well as the consistence of our Riemann surface structure, suggests that this unknown zone does not hold any surprising phenomena. Taking this for granted, our present work thus reveals, in a somehow circuitous way, some properties of a still unknown special function attached to a triple turning point, and thus new universal properties in asymptotic theory in the spirit of [19, 41].

Acknowledgments

This work has been done within the framework of the CNRS-supported 'ForMathVietNam' project, as part of the thesis of the second author, under the joint direction of the first author and of Professor F Pham. The authors are greatly indebted to Professor F Pham who introduced them to the subject and for helpful discussions, and to Professor Nguyen Huu Duc for his constant support at the University of Dalat. The second author thanks the Laboratoire J-A Dieudonné (Nice) for its hospitality and the Association d'Aubonne for financial support. He is especially grateful to Professor Nguyen Huu Duc (University of Dalat) and Professor F Pham (University of Nice) for their great financial and spiritual help.

References

[1] Bender C M, Boettcher S and Meisinger P N 1999 $\mathcal{PT}$-symmetric quantum mechanics *J. Math. Phys.* **40** 2201
[2] Bender C M and Milton K A 1998 Model of supersymmetric quantum field theory with broken parity symmetry *Phys. Rev.* D **57** 3595–608
[3] Bender C M and Boettcher S 1998 Real spectra in non-hermitian hamiltonians having $\mathcal{PT}$-symmetry *Phys. Rev. Lett.* **80** 5243
[4] Delabaere E and Pham F 1998 Eigenvalues of complex hamiltonians with $\mathcal{PT}$-symmetry I *Phys. Lett.* A **250** 25
[5] Blencowe M P, Jones H and Korte A P 1998 Applying the linear delta expansion to the $i\phi^3$ interaction *Phys. Rev.* D **57** 5092
[6] Fernández F M, Guardiola R, Ros J and Znojil M 1999 A family of complex potentials with real spectrum *J. Phys. A: Math. Gen.* 32 3105–16
[7] Znojil M 1999 Exact solution for Morse oscillator in $\mathcal{PT}$-symmetric quantum mechanics *Phys. Lett.* A **264** 108–11
[8] Znojil M 1999 Harmonic oscillator well with a screened Coulombic core is quasi-exactly solvable *J. Phys. A: Math. Gen.* **32** 4563–70
[9] Mezincescu G A 2000 Some properties of eigenvalues and eigenfunctions of the cubic oscillator with imaginary coupling constant *J. Phys. A: Math. Gen.* **33** 4911–6
[10] Cannata F, Junker G and Trost J 1998 Schrödinger operators with complex potential but real spectrum *Phys. Lett.* A **246** 219–26
[11] Caliceti E, Graffi S and Maioli M 1980 Perturbation theory of odd anharmonic oscillators *Commun. Math. Phys.* **75** 51–66
[12] Caliceti E and Maioli M 1983 Odd anharmonic oscillators and shape resonances *Ann. Inst. H Poincaré* A **38** 175
[13] Galindo A and Pascual P 1991 *Quantum Mechanics (Texts and Monographs in Physics)* (Berlin: Springer)
[14] Caliceti E 2000 Distributional Borel summability of odd anharmonic oscillators *J. Phys. A: Math. Gen.* **33** 3753
[15] Delabaere E and Pham F 1998 Eigenvalues of complex hamiltonians with $\mathcal{PT}$-symmetry II *Phys. Lett.* A **250** 29
[16] Bender C M and Wu T T 1969 Anharmonic oscillator *Phys. Rev.* **184** 1231–60
[17] Simon B 1970 Coupling constant analyticity for the anharmonic oscillator *Ann. Phys., NY* **58** 76–136
[18] Loeffel J J and Martin A 1970 *Proc. R.C.P.* no 25, vol II, Mathematics Department, Strasbourg
[19] Delabaere E and Pham F 1997 Unfolding the quartic oscillator *Ann. Phys., NY* **261** 180–218
[20] Delabaere E, Dillinger H and Pham F 1997 Exact semi-classical expansions for one dimensional quantum oscillators *J. Math. Phys.* **38** 6126–84

[21] Delabaere E and Pham F 1999 Resurgent methods in semi-classical asymptotics *Ann. Inst. H Poincaré* A **71** 1–94
[22] Voros A 1983 The return of the quartic oscillator. The complex WKB method *Ann. Inst. H Poincaré, Phys. Théor.* **39** 211–338
[23] Voros A 1993 Résurgence quantique *Ann. Inst. Fourier* **43** 1509–34
[24] Ecalle J 1984 *Cinq Applications des Fonctions Résurgentes.* Publ. Math. d'Orsay, Université Paris-Sud, 84T 62, Orsay
[25] Fedoryuk M V 1983 *Asymptotic Methods for Linear Ordinary Differential Equations* (Moscow: Nauka)
[26] Bender C M and Orszag St A 1978 *Advanced Mathematical Methods for Scientists and Engineers* (New York: McGraw-Hill)
[27] Dingle R B 1973 *Asymptotic Expansions: their Derivation and Interpretation* (Oxford: Academic)
[28] Candelpergher B, Nosmas C and Pham F 1993 Approche de la résurgence *Actualités Mathématiques* (Paris: Hermann)
[29] Berry M V and Howls C J 1991 Hyperasymptotics for integrals with saddles *Proc. R. Soc.* A **434** 657–75
[30] Olde Daalhuis A B 1998 Hyperasymptotic solutions of higher order linear differential equations with a singularity of rank one *Proc. R. Soc.* A **445** 1–29
[31] Delabaere E Un peu d'asymptotique *Pupé 28, janvier 1997, Université de Nice-Sophia Antipolis, URA 168 J.A. Dieudonné.*
[32] Koike T 1997 Perturbation series of eigenvalues of anharmonic oscillators *Exact WKB Analysis and Fourier Analysis in the Complex Domain (Kyoto, 1997)* Sūrikaisekikenkyūsho Kōkyūroku no 1001 pp 71–97
[33] Bender C M and Dunne G V 1999 Large-order perturbation theory for a non-Hermitian $\mathcal{PT}$-symmetric Hamiltonian *J. Math. Phys.* **40** 4616–21
[34] Zinn-Justin J 1989 *Quantum Field Theory and Critical Phenomena* (Oxford: Oxford Science)
[35] Delabaere E, Dillinger H and Pham F 1993 Résurgence de Voros et périodes des courbes hyperelliptiques *Ann. Institut Fourier* **43** 163–99
[36] Reed M and Simon B 1978 *Methods of Modern Mathematical Physics* vol II (New York: Academic)
[37] Colin de Verdière Y and Parisse B 1994 Equilibre instable en régime semi-classique, II: conditions de Bohr–Sommerfeld *Ann. Inst. H Poincaré* A **61** 347–67
[38] Colin de Verdière Y and Parisse B 1999 Singular Bohr–Sommerfeld rules *Commun. Math. Phys.* **205** 459–500
[39] Voros A 1999 Airy function—exact WKB results for potentials of odd degree *J. Phys. A: Math. Gen.* **32** 1301–11
[40] Voros A 1999 Exact resolution method for general 1D polynomial Schrödinger equation *J. Phys. A: Math. Gen.* **32** 5993–6007
[41] Pham F 1996 Confluence of turning points in exact WKB analysis *The Stokes Phenomenon and Hilbert's 16th Problem (Groningen, 1995)* (River Edge, NJ: World Science) pp 215–35